

Exploration Extravehicular Mobility Unit (xEMU) Lunar Boot Chamber B Thermal Vacuum Testing Results

Benjamin Swartout¹
Jacobs Technology, Houston, TX, 77058

and

Zachary Fester² and David Westheimer³
NASA Johnson Space Center, Houston, TX, 77058

NASA's Exploration Extravehicular Mobility Unit (xEMU) is the government reference next-generation spacesuit design and is engineered to protect astronauts from extreme lunar environmental temperatures. To evaluate the xEMU hardware thermal requirements, the xEMU Testing Team invented, designed, and executed a dual-suit, uncrewed thermal vacuum (TVAC) test at Johnson Space Center's (JSC) Chamber B. This paper details the test methodology, hardware setup, and results from the xEMU lunar boots. Eleven unique thermal profiles were tested including both cold and hot environmental cases over the course of five continuous days of testing. This paper will address only the cold environment testing results. The radiative thermal environment was controlled through exposure to liquid-nitrogen shrouds on the chamber walls and through a heater cage surrounding the boots. Notably, the xEMU boots also contacted the liquid-nitrogen chilled floor inside of Chamber B, which provided a conduction pathway to simulate the thermal effects of the lunar surface. Test hardware was developed to extend the water tubing from the Liquid Cooling Ventilation Garment (LCVG) into the boots to set the internal thermal boundary nominally provided by the astronaut's foot. Thirty-three temperature sensors were used to collect data in critical locations in the xEMU boot assembly as well as for calorimetry to determine heat flux to and from the boots. This paper will document the testing results and provide a high-level interpretation of the testing results. To conclude, this paper will address possible forward work and knowledge gaps present in lunar boot thermal performance and testing.

I. Introduction

NASA has spent over a decade developing spacesuit technologies for future missions, including those to the surface of the Moon. These technologies were integrated as part of the Exploration Extravehicular Mobility Unit (xEMU) and tested at the integrated spacesuit level in a series of thermal-vacuum tests in Chamber B at the Johnson Space Center (JSC)¹. One of the two spacesuit test articles evaluated was named "Suit 2," and consisted of a full Exploration Pressure Garment Subsystem (xPGS) including the boots. References 2, 3 and 4 give an overview of the Suit 2 test article and the top-level thermal results. Figure 1 shows the Suit 2 test article as it was installed in Chamber B, inside of the heater cage that was used to control the thermal environments the suit experienced. Figure 2 shows the spacesuit with a view inside of the heater



Figure 1. Suit 2 Test Article.

¹ Pressure Garment Test Engineer, Jacobs Technology, and 2101 NASA Parkway, Mail Code EC5.

² Engineering, Spacesuit and Crew Survival System Branch, 2101 NASA Parkway, Mail Code EC5.

³ Engineering, Spacesuit and Crew Survival System Branch, 2101 NASA Parkway, Mail Code EC5.



Figure 2. Suit 2 Test Article, Inside Heater Cage.

with the ground, which could be either very hot or very cold, creating a conductive heat transfer path instead of only heat exchange via radiation. In this test, it was known prior to the test that the 93K (-292°F) radiation environment was not achievable in the chamber. However, liquid nitrogen cooling to the floor was available and the boots were in contact with the floor, which enabled temperatures much closer to this lower limit.

The next aspect of boot thermal performance is that the concept of a steady state operating temperature was difficult to understand or define. In this test, the boots were in contact with the floor of the chamber that had active heat transfer, for several days without moving. Prior to the test, the team was not certain what type of cold temperatures would be achievable for the boots with this conduction interface to the floor. It was expected to be colder than the radiation environments achievable, but still likely not the 93K (-292°F). Actual temperatures in Permanently Shadowed Regions (PSR) of the lunar surface may be even colder. Exact values are not known with absolute certainty, but some requirements reviewed have been as cold as 20K (-424°F). In an actual spacesuit application, a crew member would be walking. The boots would be in contact with the lunar surface for short periods of time. Many questions existed about the thermal capacity of lunar regolith and how that will impact the heat transfer to the soles of the boots. If the regolith is loosely packed and relatively low density compared to the spacesuit, it would approach the temperature of the boots as a crew member stood in one place. If it was dense and sunk to the rocks under the regolith, the boots would sink to that temperature. Again, it is expected that a crew member would be continually moving their feet and the time for these transient thermal interactions with the lunar surface would be relatively short.

These complex boot thermal requirements for a lunar mission to locations with extreme temperatures has led to NASA identifying boot passive thermal performance as a significant technology challenge. This test was the most meaningful thermal evaluation of NASA boot concepts performed to date and provides an assessment of the thermal design of this critical component. With these important uncertainties in requirement definition, and with an understanding of the level of flight-like fidelity achievable in a test like this, the primary objective of this test was to start generating boot thermal data that could be used to

evaluate the thermal performance of the boots in the cold range of thermal environments. Boot development for lunar applications has been an area of significant technology advancement due to the challenging requirements for this application, as compared to NASA's current state of the art boots that are used for microgravity Extravehicular Activities (EVAs) at the International Space Station (ISS). Lunar boots will come into contact with lunar surface temperatures across a much wider range than seen on ISS. In addition, due to the physical contact between the boot and the surface in a partial gravity environment, thermal conduction is believed to be a bigger influence than in a microgravity mission.

II. Test Objectives

The primary objectives of this test were to evaluate xEMU hardware in space-like environments. These are primarily temperature extremes and exposure to hard vacuum pressure ($< 1 \times 10^{-5}$ Torr). xEMU thermal requirements ranged from 93K (-292°F) for a cold location on the lunar South Pole to 378K (+220°F) for a hot lunar crater. ISS thermal environments fall within that range.

Evaluating the thermal performance of a boot has some unique challenges compared to the other spacesuit components. The primary difference is that the boots are in physical contact



Figure 3. xEMU Lunar Boot.

correlate existing models, potentially provide information on transient thermal response, and simply generate a data set that could be expanded upon in future efforts. The Test Configuration section of this paper adds several important details from the test setup that aid in properly interpreting the data presented.

In addition to the thermal performance aspects of the test, simply surviving the temperature and vacuum environments without experiencing damage to the hardware was another objective of the test. Pressure garment components are primarily used in ambient pressure environment tests to evaluate design aspects like mobility, comfort, and fit. This was the most significant environmental test performed on the boots throughout their recent development.

III. Test Configuration

The generation II xEMU lunar spacesuit boots were tested during this thermal vacuum test. The Suit 2 test article was installed inside Chamber B in such a way that allowed the boots to contact the liquid-nitrogen chilled chamber floor. While the liquid-nitrogen chilled floor does provide a cold conduction pathway to the bottom of the boots, it is believed the stainless-steel chamber floor might transfer heat much more efficiently than would be expected of lunar regolith. Consequently, a second thermal insert was installed between the outsole and the chamber floor to slow the heat transfer and protect the spacesuit hardware.

A foot simulator was installed inside of the Boot Sizing Insert (BSI) that provided heat flux in the boots through temperature-controlled water lines, coiled around a sock filled with plastic pellet. The pellet provided the foot simulator with volume, to increase contact area between the water tubing and the BSI, and mass, to provide some contact force between the foot simulator and the bottom of the boot bladder. Figure 4 depicts the foot simulator. The selection of the inner diameter of the tubing was optimized around minimizing pressure drop while selecting a tubing size that could coil around the sock without the need for heat forming the tubing to reduce the bend radius. One variable that was unable to be controlled during this test was the contact force between the foot simulator and the boot bladder.



Figure 4. Foot Simulator (Top), Foot Simulator in BSI (Bottom).

The Suit 2 test article was offloaded in Chamber B from the top of the weight-relief plate on the hatch with a chain running to an I-beam. This offload system had the benefit of not blocking any view factors between the test article and the liquid-nitrogen shrouds but required careful consideration of the height and the resulting contact force between the bottom of the boots and the chamber floor. Additionally, as the chamber depressurized, the spacesuit would inflate, slightly increasing in length until the restraint lines on the softgoods were engaged. Prior to the test, evaluations took place in the xPGS Suit Lab at the Johnson Space Center where the test article was suspended, then pressurized, to characterize the increase in boot contact force as the softgoods increased in rigidity and pushed against the boots. From these evaluations, an appropriate offload height for the suit was determined. After the test article was installed in Chamber B, the spacesuit was again pressurized, while the chamber was at ambient conditions, to verify an appropriate boot contact force with the chamber floor.

In total, 33 thermocouples (TCs) were employed to measure the temperature at various locations across the boot assembly and to measure the environment conditions including both the radiation environment and the chamber floor. 27 of the 33 thermocouples were installed directly on the boot assembly and the sensor locations are documented in

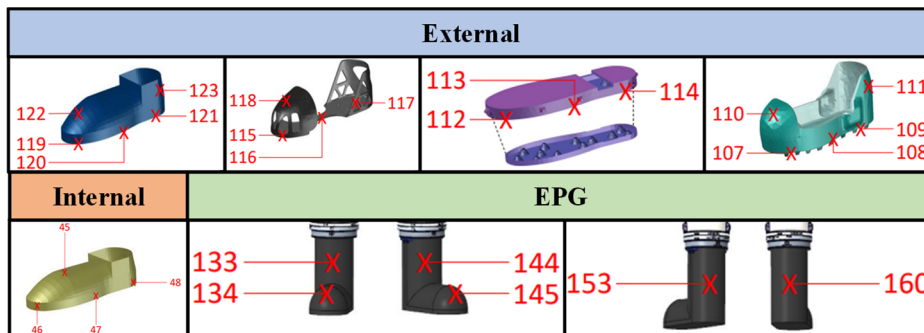


Figure 5. Thermocouple Sensor Locations.

Figure 5. The general approach in selecting TC locations was to stack the TCs through the different layers of the boot assembly and also to choose a variety of TC stack locations across the entire boot assembly.

IV. Results Summary

As aforementioned, analysis of data collected during this thermal vacuum test is on-going and this data will likely be analyzed for many years. This paper will present theories as to the performance of the lunar spacesuit boots, however firm conclusions cannot be drawn without further analysis and testing. As stated in the Test Objectives section, the dataset gathered in this test was intended to inform areas on the boot where further investigation is needed. This test was not intended to validate xEMU requirements or fully characterize spacesuit boot thermal performance. Additionally, this paper will only address the results from the cold-environment testing. At a high-level, the boots did not thermally perform as expected. The internal boot bladder temperatures were much colder than anticipated and warrants further investigation.

Previous modeling and data collected during this test indicate close coupling of temperatures between the bladder and restraint softgoods layers. Similar temperatures between the bladder and restraint layers are expected as these layers are compressed together by the internal pressure of the spacesuit. Figure 6 illustrates this. With the assumption

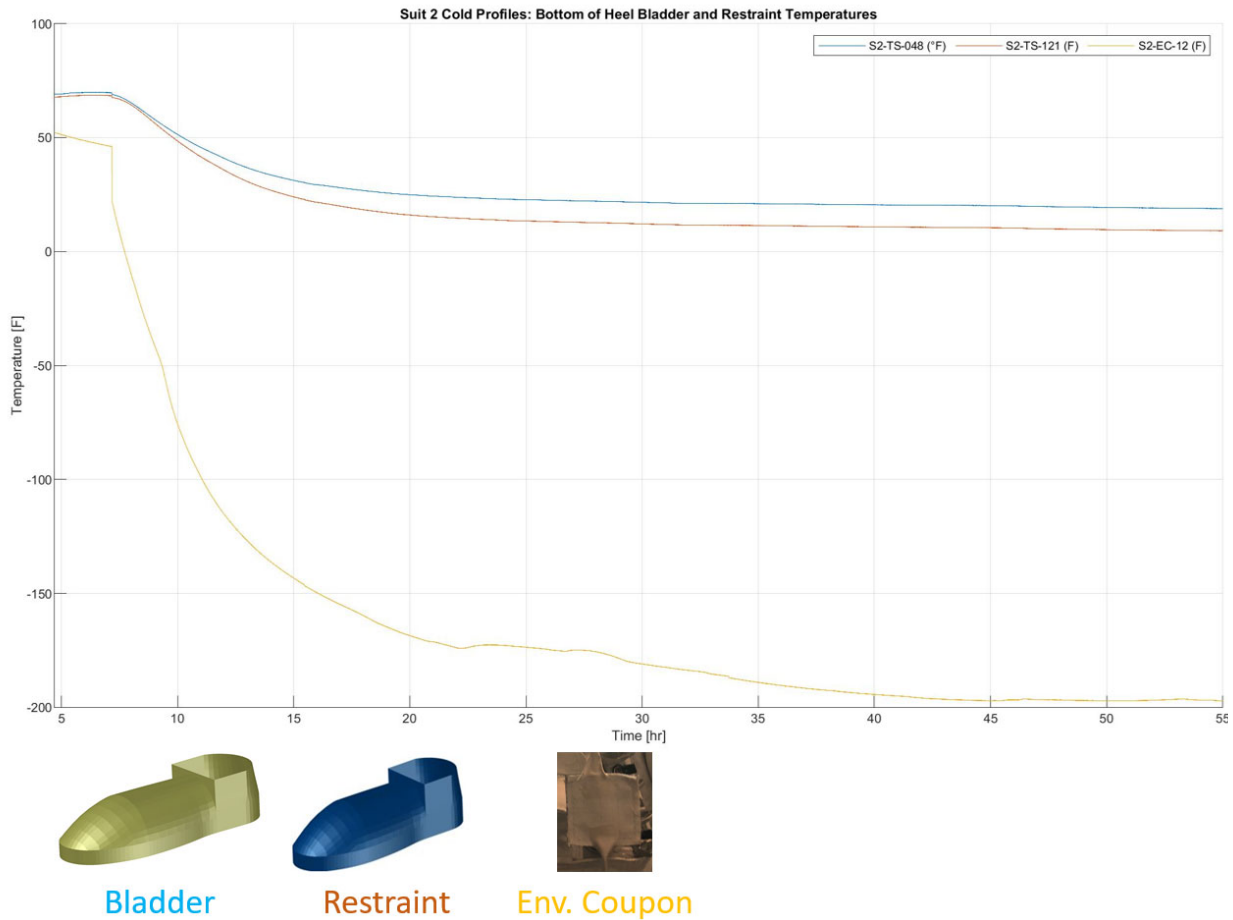


Figure 6. Bladder and Restraint Temperature Coupling.

of similar temperatures between the bladder and restraint softgoods layers validated with test data, an analysis of the restraint temperatures and consequent inference of the bladder temperatures will be considered. Figure 7 illustrates the temperature of the restraint at different sensor locations including: the top of the toe, bottom of the toe, bottom-middle of the foot, bottom of the heel, and back of the ankle. The coldest restraint temperature observed is on the back of the ankle. This is surprising as the sensor locations at the back of the ankle will experience little conductive thermal effects with the chamber floor, leaving radiative heat transfer with the environment as the primary method of heat transfer. Interestingly, the steady-state restraint temperature at the back of the ankle is quite similar to the restraint temperatures at the bottom of the toes and the top of the toes. While radiation-dominated heat transfer with the environment is expected at the top of the toes, conductive heat transfer is expected to dominate at the bottom of the

toes. The similar temperatures at these locations indicate a lack of radiation thermal insulation at multiple locations and a relatively small conductive heat transfer effect through the bottom of the boots.

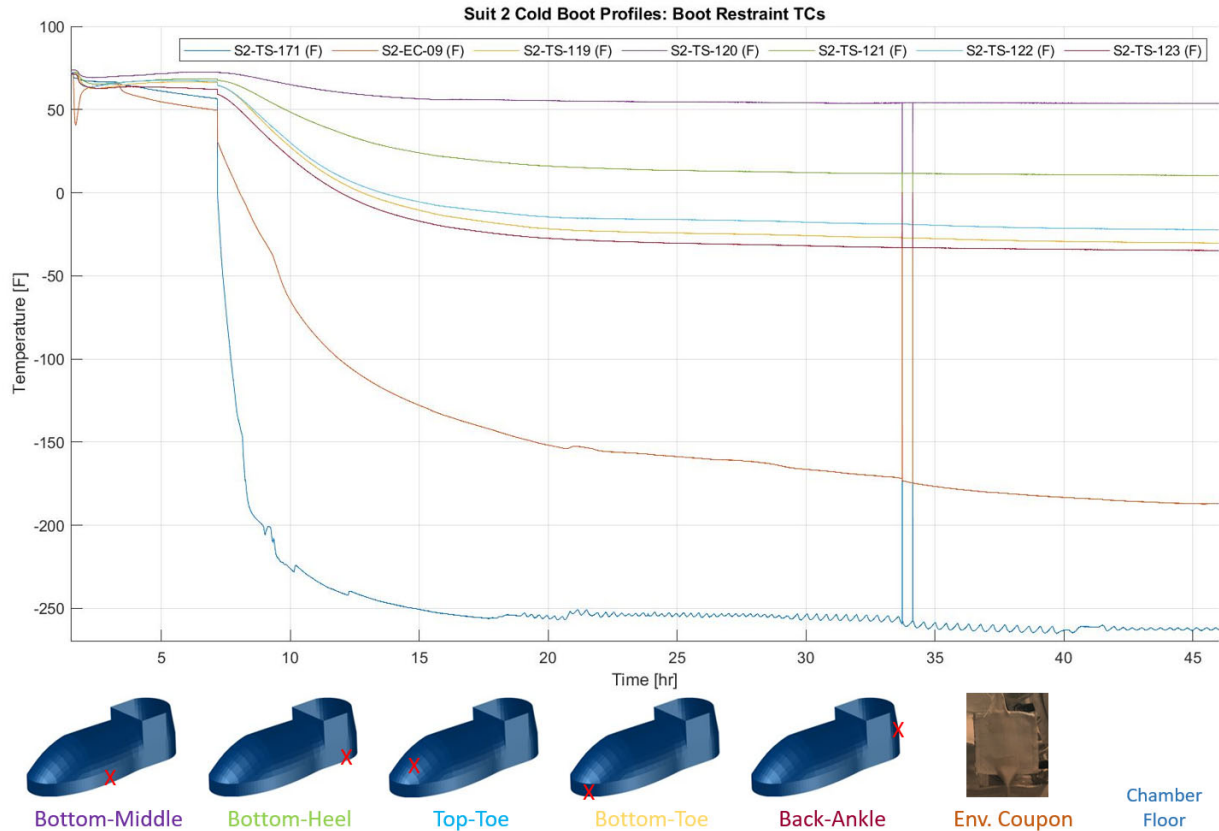


Figure 7. Lunar Boot Restraint Temperatures.

While a conduction pathway between the temperature sensor on the restraint at the back of the ankle location and the chamber floor exists through the boot outsole, it is unlikely much heat was transferred through this pathway. The outsole is constructed from thermally insulative RTV 630. Figure 8 illustrates prior modeling depicting the large temperature gradient expected along the back of the outsole, moving from the top of the heel to the bottom of the outsole.

With respect to a conduction pathway through the frame of the boot and the chamber floor, a similar conclusion is true. Figure 9 demonstrates that while the bottom-middle of the frame was 50°F, the bottom of the toes and bottom of the heel locations on the frame were around -50°F. It can be inferred from the large temperature gradient between these nearby locations on the frame that little in-plane conduction occurred. Consequently, the effect of conduction vertically from the chamber floor through the latticed frame structure to the top of the toecap and back of the ankle locations on the frame is unlikely to have significantly impacted the heat balance of the boots.

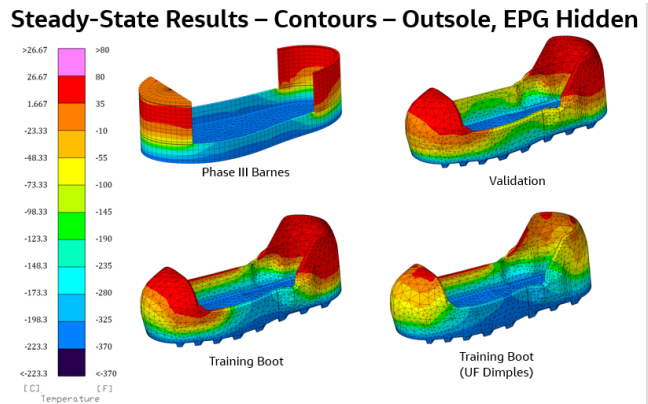


Figure 8. Model Outsole Temperature Gradient.

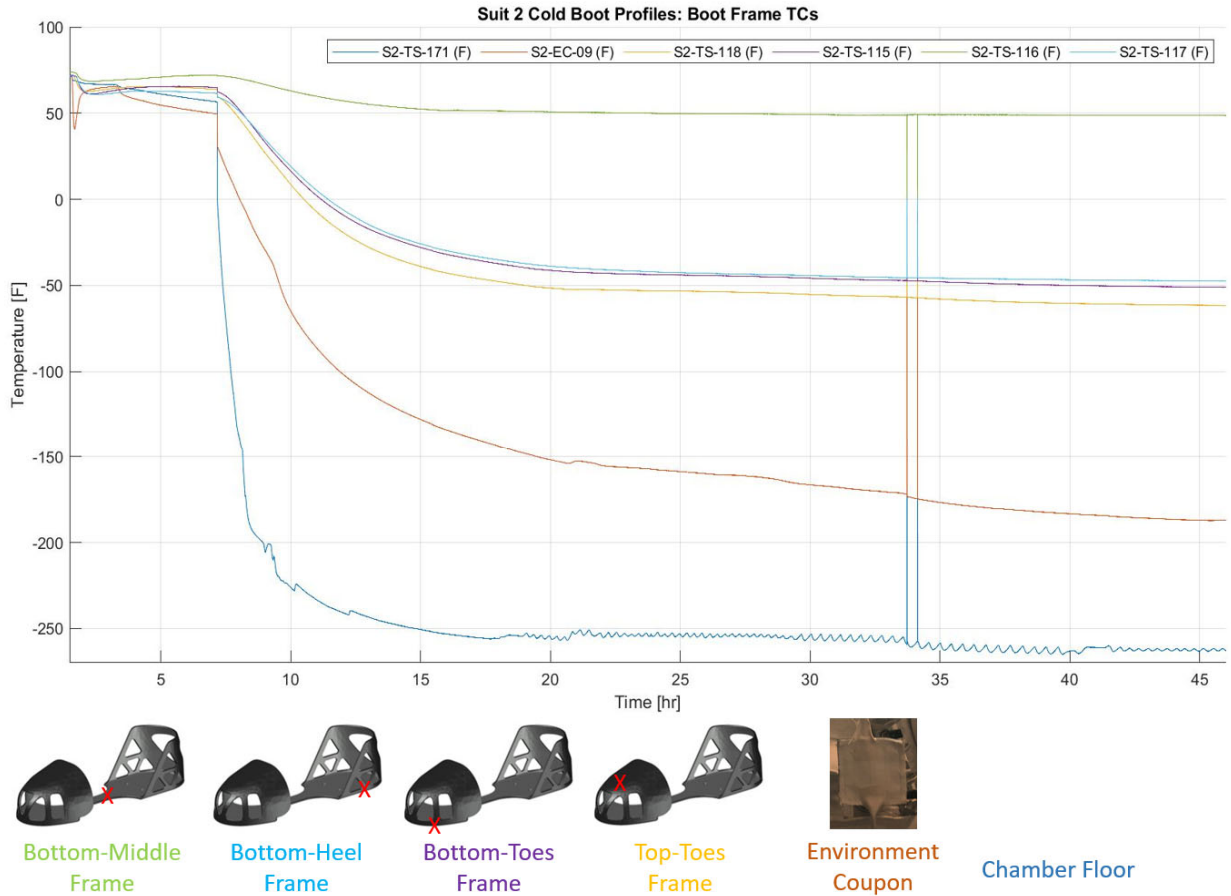


Figure 9. Boot Frame Temperatures.

Another important evaluation consideration of Figure 7 is the significant difference in temperature between the predicted temperatures and test temperatures of the restraint layer. While the boot temperatures observed during this test may not be precisely realistic to the temperatures encountered on the lunar surface, it is meaningful that a $\sim 100^{\circ}\text{F}$ delta exists between the test data and model predictions of the restraint temperatures. The restraint temperature reached below 0°F at the top of the toes, bottom of the toes, and back of the ankle locations. In comparison with other softgoods on the test article, low restraint temperatures underneath the Environmental Protection Garment (EPG) appear to be unique to the boots. As an example, Figure 10 illustrates the bladder, restraint, and EPG temperatures at the front of the right leg, near the right boot. The EPG steady state temperature is approximately -170°F , while the bladder and restraint steady state temperature are close together at $\sim 50^{\circ}\text{F}$. The large temperature delta across the EPG and warm bladder/restraint temperatures

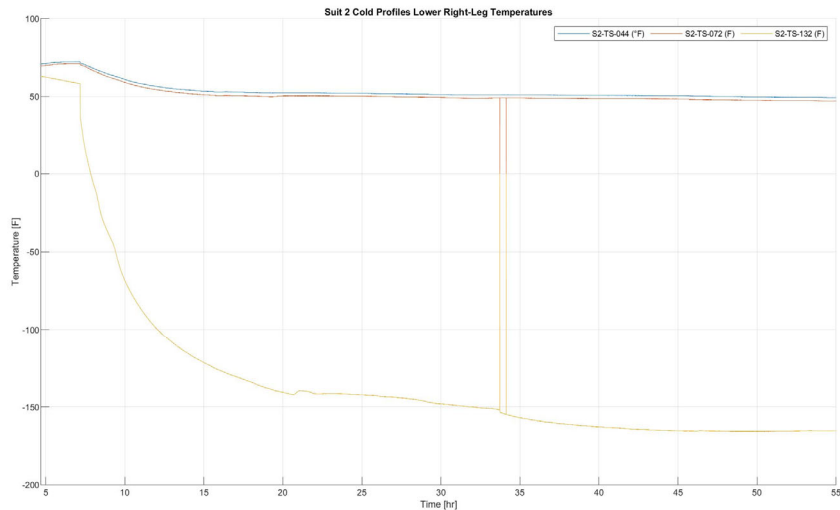


Figure 10. Lower Right Leg Temperatures.

indicates well-performing EPG thermal insulation and provides a reference of comparison for the boots as the leg was exposed to the same radiation environment as the boots. Figure 11 illustrates only a 100°F temperature delta across the EPG at the back of the ankle TC stack location on the boots where a nominal ~200°F temperature delta is expected.

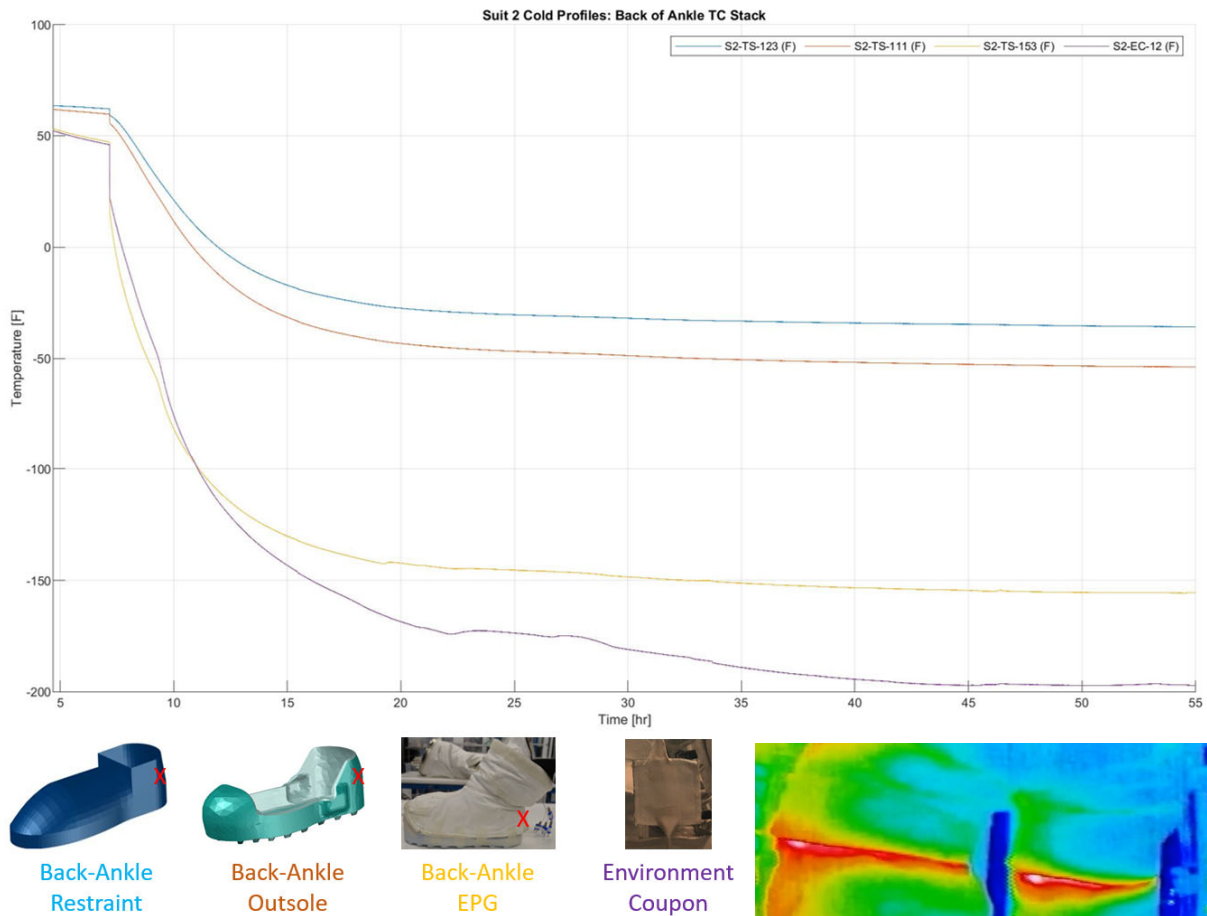


Figure 11. Back of the Ankle TC Stack.

The apparent lack of conductive heat transfer through the bottom of the boots and significant heat loss through radiative heat transfer with the environment indicates poor EPG radiation thermal insulation performance. Figure 12 visualizes the difference between boot and leg EPG performance with similar EPG insulation schemes. After the test, the right boot EPG was inspected for any factor that might contribute to insufficient multi-layer insulation (MLI) performance, i.e., damage, thermal shorts, insufficient layers of mylar, etc. The results of the inspection were inconclusive. It was found that the mylar covering the top of the toes TC stack possibly was compressed. Compressed MLI can lead to reduced effectiveness of the multiple layers of mylar. This observation is documented in Figure 13, where the mylar at the toecap appears compressed as compared to the mylar on the side of the boot (right-side in the image). Additionally, the zipper on the outward-facing side of the boot EPG and the strap on the back of the boot EPG were found to be stitched through the layers of mylar. Sewing through the mylar may cause small thermal shorts at each stitch location. However, the effects of the compressed mylar and stitching through the mylar were not characterized with this boot

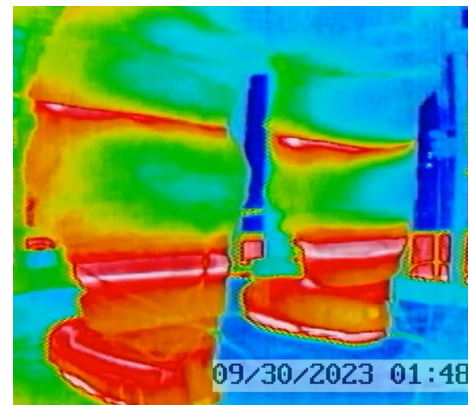


Figure 12. Cold Case Thermal Image.



Figure 13. Right Boot EPG Inspection.

EPG and the extent of heat leak contributions from these anomalies cannot be concluded. A final anomaly was discovered at the toecap of the boot. The boot EPG was intentionally terminated higher up on the toecap for mobility and wear/tear considerations during ambulation on lunar regolith. However, a gap exists between the MLI termination point and the top of the thermal insert where little to no radiation thermal insulation is present. With a view factor from the environment through this gap in insulation, the toecap is believed to be a high heat leak location. This will be considered in future EPG design iterations.



Figure 14. Boot EPG.

Table 1 summarizes the steady-state temperatures reached in the cold case. Again, it is important to remember that these temperatures are not realistic of a lunar mission and should only be considered in comparison with one another. The test article cold soaked for over 40 hours whereas a nominal EVA would last just 8 hours.

	Chamber Floor	Env. Coupon	EPG	Outsole	Thermal Insert	Frame	Restraint	Bladder
Top of Toes	-263°F	-172°F	-132°F	-73°F	N/A	-62°F	-23°F	54°F
Bottom of Toes		N/A	N/A	-128°F	-120°F	-51°F	-31°F	-53°F
Bottom-Middle of Foot		N/A	N/A	-100°F	-94°F	48°F	53°F	63°F
Bottom of Heel		N/A	N/A	-115°F	-104°F	-48°F	9°F	19°F
Back of Ankle		-197°F	-164°F	-53°F	N/A	N/A	-35°F	N/A

Table 1. Max Cold Boot Steady State Results Summary.

One interesting finding is the difference in radiation environments between the front and back of the test article. This is explained by the back of the spacesuit having a direct view factor to the liquid-nitrogen shrouds on the chamber walls whereas the front of the suit faced a mylar divider separating the two test articles. It is believed that radiated heat from the front of the test article reflected off of the mylar divider and back onto the test article. Table 1 illustrates the back of the ankle location on the boot had an environment coupon steady-state temperature at -197°F while the top of the toe location on the boot had an environment coupon steady-state temperature at -172°F. The front and back of the boot experienced around a 25°F temperature difference in their radiation environments. The effects of the different radiation environments can be observed in the top of the toes and back of the ankle TC stack location on the boot. At these locations, radiative heat transfer with the environment is expected to be the primary pathway for heat leak. The EPG and restraint layer at the back of the ankle experienced colder temperatures than at the top of the toes location on the boot. While this finding tracks well with the colder environment on the back of the test article, one contributing factor to the temperature delta in addition to the different radiation environments is the gap in the boot frame at the back of the ankle location. At the back of the ankle, the restraint is likely in direct contact with the outsole as there is a gap in the lattice structure of the boot frame. At the top of the toes location, heat must transfer through the frame structure from the restraint layer to the outsole, adding an additional thermal resistance to the heat balance at that location.



Figure 15. Mylar divider between the test articles.

In regard to the thermal insert, it is difficult to characterize thermal performance. An additional thermal insert was added between the outsole of the boot and the chamber floor for this test, as the liquid-nitrogen chilled floor was expected to transfer heat much more efficiently than lunar regolith. For this reason, the second thermal insert was added to slow the heat transfer and protect the spacesuit hardware,

while still providing a conduction pathway that could be characterized through a combination of test data analysis and model simulations matching the test setup. As discussed previously in this paper, it appears that many locations on the boot experienced significant heat loss with the environment through the EPG and those locations are therefore not good candidates to assess the conductive thermal insulation performance of the thermal insert. However, the TC stack location at the bottom-middle of the foot was insulated from the environment by the foot simulator inside the boot and it is believed this sensor location had minimal view factors to the environment through the EPG. Figure 17 illustrates the temperatures of the boot layers at this location. Notably, a $\sim 150^{\circ}\text{F}$ temperature delta is observed between the bottom of the thermal insert and the frame, which indicates encouraging performance of the thermal insert. The thermal insert performance relies on decreasing contact area with the outsole by incorporating small standoffs to slow the conductive heat transfer. Between the top and bottom of the thermal insert, mylar is added across the entire thermal insert, essentially suspended on the wedge shape of the standoffs. Much of the heat transfer between the bottom of the outsole and the boot softgoods is radiative heat transfer through the mylar layers in the thermal insert, with some conduction effects through the standoffs. With this architecture in mind, the temperature delta across the thermal insert is expected to increase as the temperature of the bottom of the outsole decreases. A large temperature delta across the thermal insert in this test is encouraging that the thermal insert might perform well if exposed to lunar PSR temperatures, however testing PSR thermal environments and better characterizing the heat transfer through bottom of the boot remains forward work.

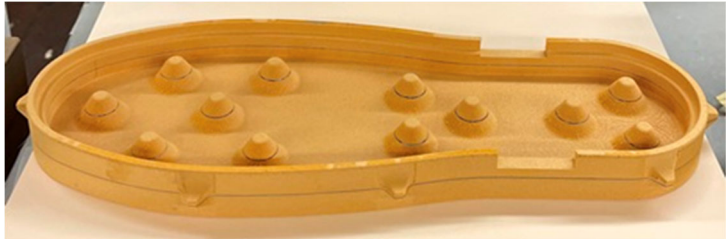


Figure 16. Boot Thermal Insert. (Mylar not shown).

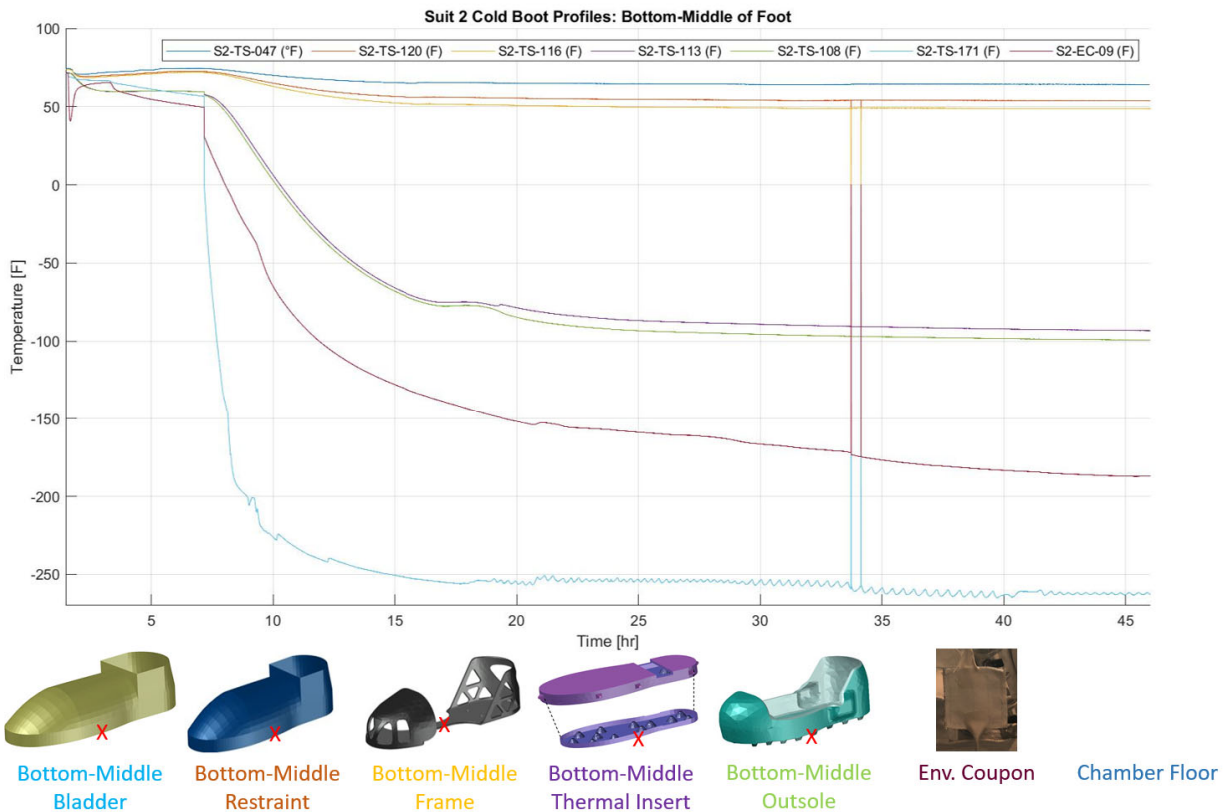


Figure 17. Bottom-Middle of Foot Temperatures.

Figure 18 illustrates the bladder, restraint, and EPG temperatures at the boot bearing. The steady-state temperature of the internal and external metallic surfaces of the bearing was around 35°F , with the internal surface slightly warmer than the external surface. The EPG temperature was around -170°F , and the plot depicts an approximate 200°F temperature delta across the EPG, similar to the observed temperature delta across the EPG for the lower right leg.

While an internal steady-state temperature of 35°F is slightly below the lower internal touch temperature requirement of 50°F, it is within the correct order of magnitude of acceptability, and it is likely the bearing temperature would rise within acceptable limits with higher-fidelity testing. With the proposed theory of ineffective EPG on the boot, it would be expected that the boot bearing would also experience significant heat loss to the environment. The relatively warm boot bearing temperatures as compared with the rest of the boot can be attributed to the overlapping EPG interface between the leg and boot EPG pieces. Nominally performing MLI on the leg EPG piece covered the boot bearing.

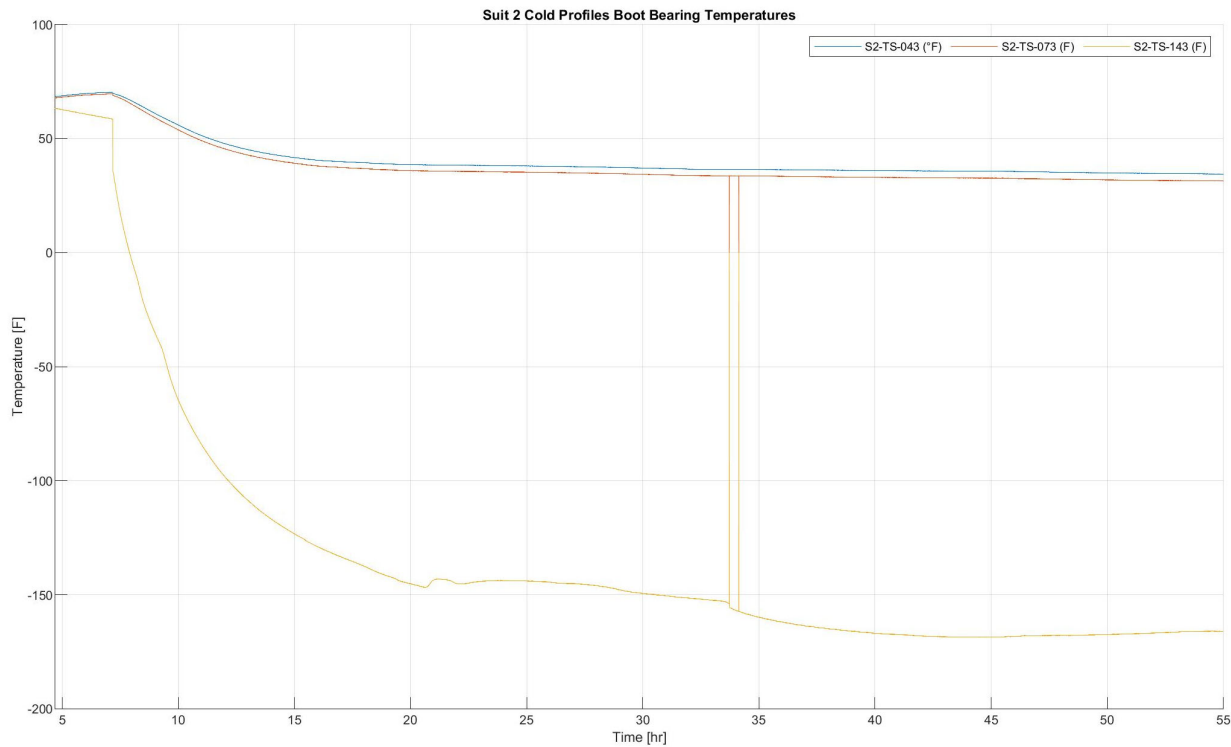


Figure 18. Boot Bearing Temperatures.

V. Lessons Learned

Thermal testing of lunar spacesuit boots is challenging. This thermal vacuum test evaluated the overall performance of the boots, however no opportunities existed to change variables to better characterize thermal performance of individual layers of the boot assembly. As an example discussed in the paper, it is difficult to make quantitative conclusions about the distribution of heat leak through the EPG and through the bottom of the boots. It is also difficult to compare the results gathered during this test to ISS and lunar environments. The radiation environment in the chamber was warmer than will be experienced in LEO or at the lunar South Pole. Furthermore, while the liquid-nitrogen chilled chamber floor did provide a conduction pathway with the bottom of the boots, the chamber floor was likely more aggressive than the lunar surface will be. Forward work remains in modeling the test setup given the data collected during the test to better inform the nominal boot thermal model for LEO and lunar environments.

While a low-fidelity foot simulator was sufficient for assessing the high-level thermal performance of the spacesuit boots, it is interesting to consider what it means to have a high-fidelity foot simulator. The foot is difficult to simulate as it has a complicated architecture and variance in heat generation, volume, mass. Adding to this complexity is the subjective nature of boot sizing. Some test subjects prefer a tight boot fit while others prefer a loose boot fit. A tighter boot fit might increase the contact force between the foot and boot bladder while a loose boot fit might allow more motion of the foot inside the boot and better distribute heat across the entire bottom surface of the boot bladder. With all of these variables in mind, thermal modeling of the xEMU boot is a powerful tool. With better characterization of the thermal performance of individual boot softgoods layers and insulation schemes in future testing, the xEMU boot thermal model can be validated and accurately predict boot thermal performance while accounting for the numerous aforementioned variables.

This thermal vacuum testing was important as it highlighted that further investigation and testing is needed to better understand the thermal performance of the xEMU boots. While this boot thermal test did not have the same fidelity as a certification-level test, it was successful in identifying areas of risk with the xEMU boot design and gave insights into design of future lunar boot thermal testing.

A knowledge gap that remains after this thermal vacuum testing of the xEMU boot is spacesuit boot thermal performance in Permanently Shadowed Regions (PSRs). The xEMU spacesuit has a two-hour exposure time requirement in a PSR where temperatures can reach down to -380°F, and this requirement drives the thermal insulation design scheme of the boot. Little test data exists for how the boot might perform in a PSR environment and remains a risk for spacesuit development in the future.

VI. Conclusion

The xEMU project produced high fidelity spacesuit hardware and successfully tested it in a space-like environment. This test series serves as an excellent reference design for future spacesuit development efforts to build from. Not only did the hardware perform well, but this unique spacesuit test can be a reference for future demonstrations.

Acknowledgments

This work was funded by the EVA and Human Surface Mobility Program. Special recognition goes to Martin Carrasco and Darryl Moore for designing and building the heater cage. Thermal analysts Chane Sladek, Michael Lewandowski, Noah Andersen, and Monica Mah supported testing operations in addition to the authors of the paper. Chane Sladek provided pre-test thermal analysis. Brad Butler, Gabe Bernal, Bill Foster, Alan Turner, Steve Smith, and Felipe Zapata all provided the expertise and ground effects lights that made the test possible. The Suit 2 test team of Kathryn Bock, Henna Calderon, and Jaren Grimes helped provide around the clock test support. The Systems Test Branch personnel that ran the chamber and directed the test also did an exceptional job. PGS team support including build up and assembly assistance from technicians Kevin Groneman and Pete Meeh; as well as inspiration, guidance, mentorship, and motivation from team managers Richard Rhodes and Don Campbell were invaluable.

References

¹Westheimer, D., Rodrigues, L., Falconi, E., Swartout, B., and Lewandowski, M., “xEMU Thermal Vacuum Testing Overview,” International Conference on Environmental Systems, ICES, Louisville, KY, 2024.

² Swartout, B., and Westheimer, D., “Exploration Extravehicular Mobility Unit (xEMU) Chamber B Thermal Vacuum “Suit 2” Pressure Garment System Hardware and Test Design,” International Conference on Environmental Systems, ICES, Louisville, KY, 2024.

³Swartout, B., “Exploration Extravehicular Mobility Unit (xEMU) Chamber B Thermal Vacuum “Suit 2” Pressure Garment System Test Article Results,” International Conference on Environmental Systems, ICES, Louisville, KY, 2024.

⁴Fester, Z. and McFarland, S., "NASA Advanced Space Suit xEMU Development Report – Lunar Boots." In: 51st International Conference on Environmental Systems. 2022.